

## Excitation and Probing of Infrared Nanoantenna Modes under Oblique Illumination

\*Shuta Kitade<sup>1)</sup>, Shingo Usui<sup>2)</sup>, Ikki Morichika<sup>1)</sup>, Kensuke Kohmura<sup>2)</sup>, Fumiya Kusa<sup>2)</sup> and Satoshi Ashihara<sup>1),2)</sup>

Institute of Industrial Science, The University of Tokyo<sup>1)</sup>, Department of Applied Physics, Tokyo University of Agriculture and Technology<sup>2)</sup>  
E-mail: skitade@iis.u-tokyo.ac.jp

We study near-field distributions of infrared nanoantennas under oblique illumination. We obtain the amplitude- and phase-resolved images of the near-fields on Au nanoantennas by use of the scattering-type scanning near-field optical microscopy. Resonant excitation of the 1st-order (dipole) mode and that of the 2nd-order (quadrupole) mode, and their asymmetric near-field distributions are experimentally visualized and numerically reproduced.

### 1. Introduction

Nanoantennas resonating at mid-IR range are gaining great attention because of their attractive potential for surface-enhanced vibrational spectroscopy<sup>1)</sup>, chemical/bio sensing<sup>2)</sup> and nonlinear light-matter interactions<sup>3)</sup>, etc.

In practical applications, antenna excitation may be spatially inhomogeneous because of oblique illumination, structured wave-front, etc. Therefore, it is crucial to elucidate excitation properties and near-field distributions of nanoantenna modes for such excitation conditions.

Here we experiment and study excitation properties and near-field distributions of surface plasmon modes on Au nanoantennas under oblique illumination.

### 2. Experiment

The IR-resonant Au nanoantennas are fabricated on a SiO<sub>2</sub>-glass substrate by the electron beam lithography and the lift-off process. The nanoantennas have a common width of 200 nm, a common height of 30 nm, and varied length  $L$ 's of 2.2, 2.8, 3.4, 4.0, 4.6, 5.2, and 5.8  $\mu\text{m}$ . The antennas are illuminated at oblique incidence (an incidence angle of 60°) and with p-polarization, as shown in Fig.1. Amplitude- and phase-resolved images are obtained by our developed scattering-type scanning near-field optical microscopy (s-SNOM)<sup>4)</sup> with interferometric homodyne detection.

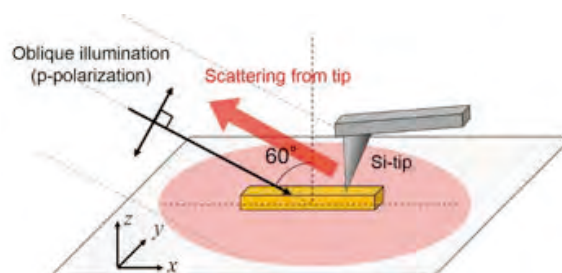


Fig.1 Geometry for nanoantenna excitation and near-field detection.

### 3. Results

Figure 2 summarizes the measurements for the nanoantenna of  $L = 2.8 \mu\text{m}$ , namely, (a) the amplitude image, (b) its line profile, (c) the phase image, and (d) its line profile. Figure 2 (e)-(h) display that simulation results. One can find that there are two bright regions separated by a dark region (a single node), and that the phase has a stepwise profile with a jump of  $\pi$  at the node. Such amplitude- and phase-distributions indicate the 1st-order (or dipole) antenna mode. One can clearly see that the amplitude profile is spatially asymmetric. These features are perfectly reproduced in the numerical simulations.

Figure 3 summarizes the measurements for the nanoantenna of  $L = 5.8 \mu\text{m}$ , similar to the ones shown in Fig.2 for  $L = 2.8 \mu\text{m}$ . One can find that there are three bright regions separated by two nodes, and that the phase has a stepwise profile with two jumps of  $\pi$ . Such amplitude- and phase-distributions indicate the 2nd-order (quadrupole) antenna mode. Again, the asymmetric amplitude profile is clearly observed. These features can be seen in the numerical calculations.

The asymmetry in the near-field distributions is attributed to the preferential excitation of the surface plasmon polariton (SPP) in one direction and the finite loss of the SPP inside the nanoantennas. We will also discuss the excitation conditions at oblique illumination in the presentation.

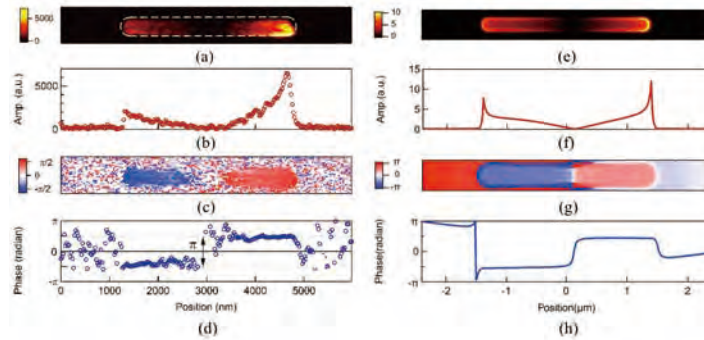


Fig.2 The measured and simulated data for the Au nanoantenna of  $L = 2.8 \mu\text{m}$ : (a, e) the amplitude image, (b, f) its line profile, (c, g) the phase image, and (d, h) its line profile.

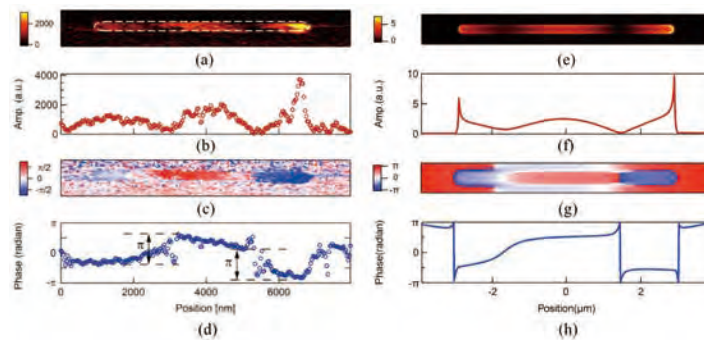


Fig.3 The measured and simulated data of the Au nanoantenna of  $L = 5.8 \mu\text{m}$ .

#### 4. Conclusion

In summary, we obtain amplitude- and phase-resolved images of the near-fields by using our developed s-SNOM and the interferometric homodyne detection. Resonant excitation of the 1st-order (dipole) mode and that of the 2nd-order (quadrupole) mode are observed for the nanoantenna with different lengths. Asymmetric near-field distributions are experimentally visualized and numerically reproduced. In addition, we organize the excitation conditions of the nanoantenna modes in terms of the cavity resonance condition and the phase matching condition for SPP in the nanoantenna.

#### Reference

- 1) F. Neubrech, *et al.*, "Surface-Enhanced Infrared Spectroscopy Using Resonant Nanoantennas," *Chem. Rev.* **2017**, *117*, 5110" 5145.
- 2) C. V. Hoang, *et al.*, "Monitoring the Presence of Ionic Mercury in Environmental Water by Plasmon-Enhanced Infrared Spectroscopy," *Sci. Rep.* **2013**, *3*, 1175.
- 3) F. Kusa, *et al.*, "Optical Field Emission from Resonant Gold Nanorods Driven by Femtosecond Mid-Infrared Pulses," *AIP Adv.* **2015**, *5* 077138.
- 4) R. L. Olmon, *et al.*, "Near-Field Imaging of Optical Antenna Modes in the Mid-Infrared," *Opt. Express* **2008**, *16*, 20295-20305.